PAPER REFERENCE: 10V.282

HYDROGEN ASSISTED CRACKING OF COLD DRAWN EUTECTOID STEEL FOR CIVIL ENGINEERING STRUCTURES

J. Toribio and E. Ovejero

Department of Materials Science, University of La Corufia,
ETSI Caminos, Campus de Elvifia, 15192 La Corufia, Spain

ABSTRACT

This paper analyzes the hydrogen assisted cracking (HAC) behaviour of cold drawn prestressing steels with different degrees of cold drawing. The experimental results showed a progressively anisotropic behaviour as the degree of cold drawing increases, with an evolution in the fracture behaviour from mode I (isotropic behaviour in slightly drawn steels) to mixed mode propagation (strongly anisotropic behaviour in heavily drawn steels). The fractographic analysis revealed changes in the microscopic topography depending on the fracture propagation mode, with an evolution from pure ***tearing topography surface*** (TTS) in slightly drawn steels to a kind of ***very*** *deformed* TTS in heavily drawn steels. The role of microstructural orientation induced by cold drawing in these fractographic appearances is discussed, as well as its influence on the macroscopic change of crack propagation direction in progressively drawn steels. A micromechanical model for the initiation and propagation of hydrogen-assisted subcritical cracking is suggested. It accounts for the phenomenon of shear cracking (SC) in the pearlitic lamellae according to the micromechanism proposed by Miller & Smith, and considers the deleterious effect of the hydrogen presence on the appearance of the critical event by a micromechanism of hydrogen enhanced delamination (HEDE).

INTRODUCTION

Cold drawn eutectoid steels are high-strength materials used as constituents of prestressed concrete structures in civil engineering. In these steels, the manufacturing process by cold drawing produces a marked orientation of the pearlitic microstructure of the steel at the levels **of** pearlitic colonies and lamellae [1–6], inducing strength anisotropy. Thus, although cold drawing improves the mechanical properties of the steel, the microstructural changes during manufacture may affect dramatically its environmentally assisted cracking performance and this is potentially dangerous when the engineering structures work in aggressive environments [7-9]. This paper analyzes the hydrogen assisted cracking (HAC) behaviour of cold drawn prestressing steels with different degrees of cold drawing, to elucidate the influence of the strain hardening level on the HAC phenomenon, an important particular case of stress corrosion cracking (SCC).

EXPERIMENTAL PROGRAMME

The materials used in this work were high-strength steels taken from a real manufacturing process. Wires with different degrees of cold drawing were obtained by stopping the manufacturing chain and taking samples from the intermediate stages. The different steels were named with digits 0 to ***6*** which indicate the number of cold drawing steps undergone. Table 1 shows the chemical composition common to all steels, and Table 2 includes the diameter (D_i), the yield strength (σ_Y), the ultimate tensile stress (OR) and the fracture toughness (K_{IC}).

To analyze the HAC behaviour of the different steels, slow strain rate tests were performed on precracked steel wires. Samples were precracked by axial fatigue in the normal laboratory air environment to produce a transverse precrack, so that the maximum stress intensity factor during the last stage of fatigue precracking was $K_{max} = 0.30K_{IC}$, and the crack depth was $a = 0.30D$ in all cases, with D as the wire diameter. After precracking, samples were placed in a corrosion cell containing aqueous solution of 1g/l $Ca(OH)_2$ plus 0.1g/l NaCl (pH=12.5) The experimental device consisted of a potentiostat and a three-electrode assembly. All tests

were conducted under potentiostatic control at −1200 mV vs. SCE at which the SCC mechanism is HAC [9]. The applied displacement rate in axial direction was constant during each test and proportional to each wire diameter: 1.7×10^{-3} mm/min for steel 6 and 3.0×10^{-3} mm/min for steel 0.

TABLE 1
CHEMICAL COMPOSITION (wt %) OF THE STEELS

C	Mn	Si	P	S	Cr	V	Al
0.80	0.69	0.23	0.012	0.009	0.265	0.060	0.004

TABLE 2
DIAMETER REDUCTION AND MECHANICAL PROPERTIES OF THE STEELS

Steel	0	1	2	3	4	5	6
D_i (mm)	12.00	10.80	9.75	8.90	8.15	7.50	7.00
σ_Y (GPa)	0.686	1.100	1.157	1.212	1.239	1.271	1.506
σ_R (GPa)	1.175	1.294	1.347	1.509	1.521	1.526	1.762
K_{IC} (MPam$^{1/2}$)	60.1	61.2	70.0	74.4	110.1	106.5	107.9

EXPERIMENTAL RESULTS

In Fig. 1 a plot is given of the time to final fracture in the tests, as well as the susceptibility of the different steels to HAC, evaluated as the ratio of the fracture load in the HAC test F_{HAC} to the fracture load in air F_0. The results show no clear trend in the matter of susceptibility to HAC as a function of the degree of cold drawing (expressed by the ratio D_i/D_0), i.e., no significant improvement is detected in the fracture resistance of the steels as a consequence of the cold drawing process when the environmental mechanism is hydrogen embrittlement. However, a certain drawing-induced increase of time to failure seems to exist, *so* the steel performance is slightly better in the cold drawn prestressing steel wire than in the hot rolled bar.

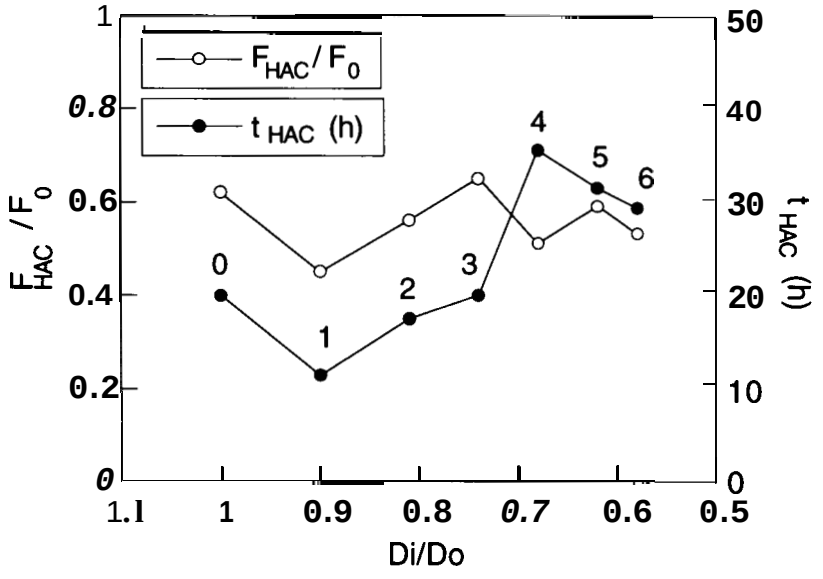

Figure 1: Fracture load in HAC conditions (F_{HAC}) divided by the fracture load in air (F_0) and time to fracture in the environment-sensitive cracking tests (t_{HAC}).

Fig. 2 shows the evolution of the fracture profile in HAC as the degree of cold drawing increases. In the first steps of cold drawing (specimens 0 and 1) the crack growth develops in mode I in both fatigue precracking and HAC. In steels 2 and 3 there is a slight deflection in the hydrogen-assisted crack. For the most heavily drawn specimens (4 to ***6)*** the crack deflection takes place suddenly after the fatigue precrack and the deviation angle is even higher. In these last stages of cold drawing, not only crack deflection but also crack branching is observed just after the fatigue precrack tip, i.e., there are two pre-damage directions (crack ***embryos),*** only one of which becomes the final fracture path. A mode **I** propagation distance associated with subcritical crack growth by HAC appears only in the first stages of cold drawing, since in heavily drawn steels crack deflection takes place just at the fatigue precrack and thus the mode I propagation distance is zero.

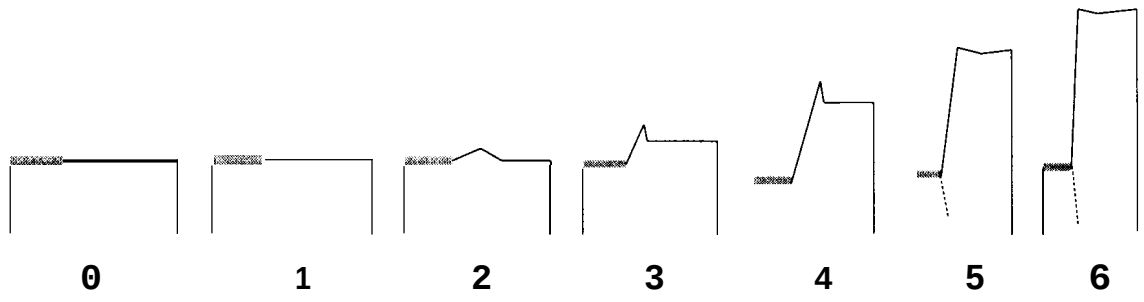

Figure 2: Fracture profile of the different steels in the HAC tests.

FRACTURE MECHANICS APPROACH

A fracture mechanics approach is presented in this section to evaluate a ***characteristic*** (or ***critical)*** stress intensity factor associated with the ***transition*** from the subcritical regime of HAC to the critical regime of environmentally unassisted fracture by cleavage. This ***transition stress intensityfactor*** is a fundamental issue in engineering design against environmentally assisted fracture. To obtain it, an expression is required of the stress intensity factor K_I for the geometry and loading mode under consideration: a cylinder in tension with an edge crack perpendicular to the tensile loading direction. The following expression [10] was used:

$$K_I = M(\xi)\,\sigma\sqrt{\pi a} \qquad (1)$$

where σ is the remote axial stress, ***a*** the crack depth and $M(\xi)$ a dimensionless function given by:

$$M(\xi) = (0.473 - 3.286\,\xi + 14.797\,\xi^2)^{1/2}\,(\xi - \xi^2)^{-1/4} \qquad (2)$$

where ξ is the ratio a/D of the crack depth to the sample diameter. This function comes from the computation —by the compliance method— **of** the global energy release rate in the considered geometry and loading mode.

This approach is only valid to establish quantitative relationships in slightly drawn steels in which the fracture process develops in mode I in the subcritical and critical regimes. The crack deflection which takes place in heavily drawn steels produces a mixed mode stress state (with an important mode II component) so that the computation of stress intensity factors is an extremely difficult task out of the scope of this paper, since there is not only K_I but also K_{II} during the subcritical crack growth.

The transition stress intensity factor K_{HAC} for HAC may be calculated **as** follows:

$$K_{HAC} = M\,(a_{fat} + x_{HAC})\,\sigma_{HAC}\sqrt{\pi\,(a_{fat} + x_{HAC})} \qquad (3)$$

where a_{fat} is the fatigue precrack (that existing at the beginning of the HAC test), x_{HAC} the depth of subcritical crack growth by HAC in mode I, and σ_{HAC} the remote stress at the critical instant of the HAC tests (maximum value), i.e., $\sigma_{HAC} = 4F_{HAC}/\pi D^2$, F_{HAC} given in Fig. 1.

The ratio K_{HAC}/K_{IC} (where K_{IC} is the fracture toughness, cf. Table **2)** allows a fracture mechanics evaluation of the HAC susceptibility of each steel. Fig. **3** shows such a susceptibility as a function of the degree of cold drawing D_i/D_0. A remarkable decrease of fracture resistance of the steels in cathodic conditions is observed, since the critical stress intensity factor in hydrogen is clearly lower than the fracture toughness of the steels in air, i.e., in the absence of any aggressive environment.

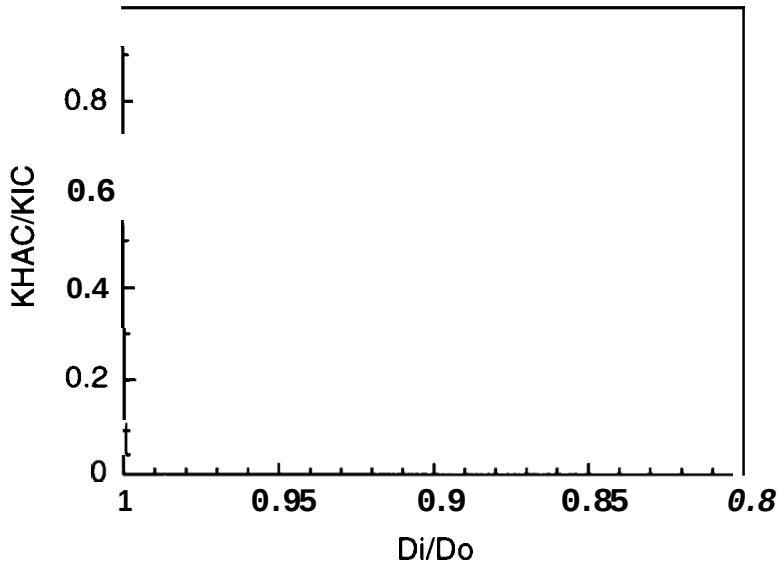

Figure 3: Susceptibility of slightly drawn steels to **HAC,** evaluated as the ratio of the critical stress intensity factor in **HAC** K_{HAC} to the fracture toughness in air K_{IC}, as a function of the degree of cold drawing D_i/D_0.

FRACTOGRAPHIC ANALYSIS

Macroscopic Appearance of the Fracture Surfaces

As shown in the fracture profiles given in Fig. **2,** the fracture behaviour in conditions of **HAC** is increasingly anisotropic with cold drawing. Fig. **4** gives the definition of parameters which quantify the evolution with cold drawing of the macroscopic crack path.

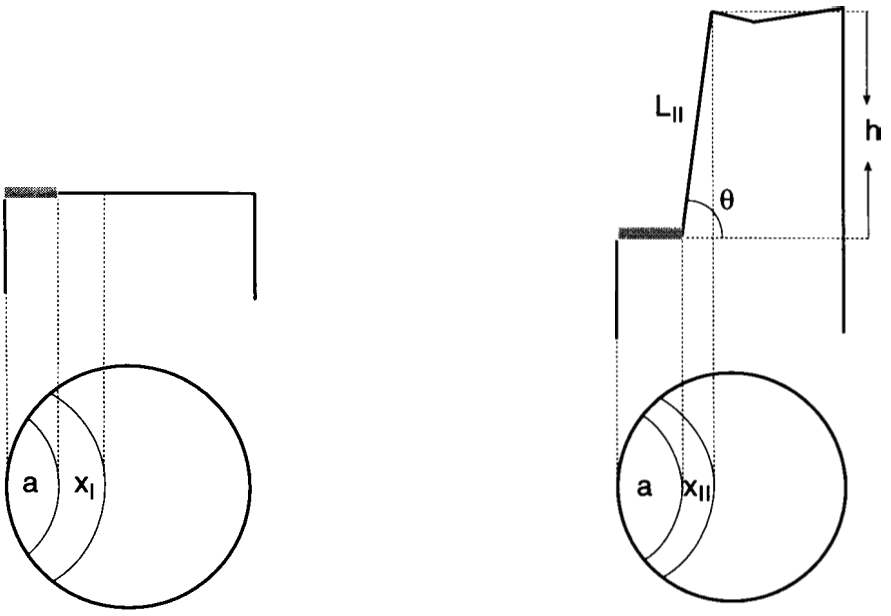

Figure 4: Definition of geometric parameters of the macroscopic crack path: (a) subcritical mode I propagation distance in slightly drawn steels 0 and 1; (b) crack growth distances and deflection angle in heavily drawn steels **2** to 6; ***a*** is the fatigue crack depth.

The evolution with cold drawing of the measured geometric parameters associated with the macroscopic crack path are given in Figs. ***5*** and 6 which show an increasingly anisotropic trend, i.e., the crack deflection angle θ, the propagation step height h and the mode II crack growth length L_{II} increase with cold drawing.

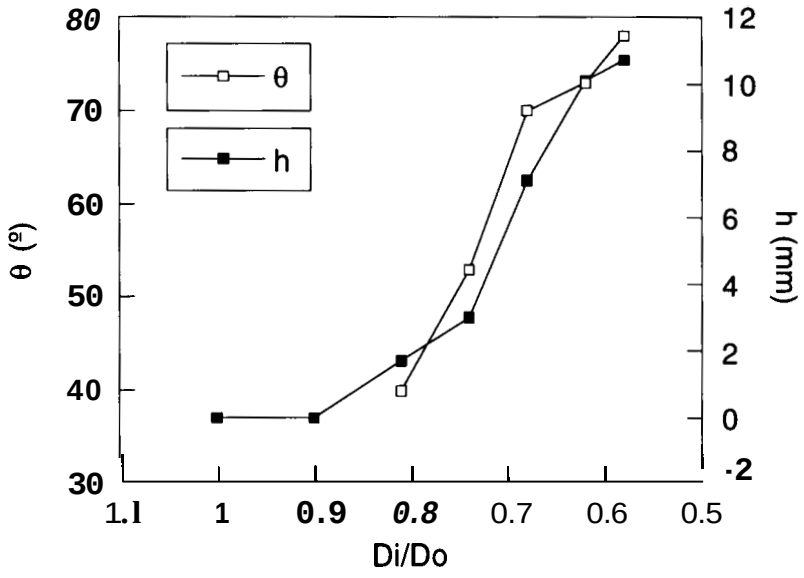

Figure 5: Crack deflection angle θ and propagation step height h (cf. Fig. 4).

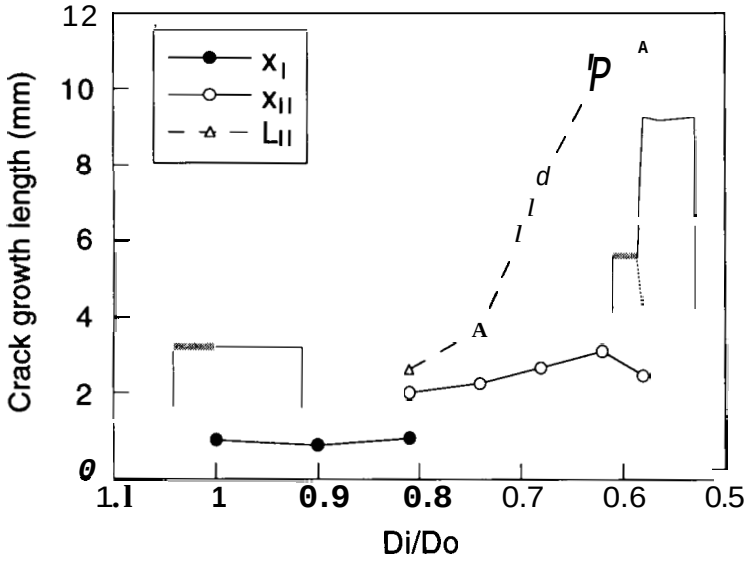

Figure 6: Subcritical crack propagation distances (cf. Fig. 4).

Microscopic Modes of Fracture

A fractographic analysis by scanning electron microscopy **(SEM)** was carried out on the fracture surfaces to elucidate the microscopic modes of fracture. Figs. 7 and **8** offer respectively the microscopic topographies for **a** slightly drawn steel (number 1 which has undergone only one step of cold drawing) and for a heavily drawn steel (number 5 which has suffered five steps of cold drawing).

In slightly drawn steel 1 (Fig. 7) there is a subcritical crack growth in mode **I** by *tearing topography surface* (TTS, cf. [11-15]) before the unstable cleavage-like propagation associated with mechanical final fracture. This special microscopic fracture mode is undoubtedly associated with hydrogen-assisted micro-damage in steels with pearlitic microstructure [13-15].

In heavily drawn steel 5 (Fig. **S)** the microscopic fracture mode is a kind of *very deformed* TTS, the deformation axis coincident with the cold drawing direction. This topography is produced as a consequence of

the macroscopic crack deflection with mode II propagation, i.e., as if a previous **TTS** mode had been strained by shear in its own fracture plane (quasi-parallel to the drawing axis).

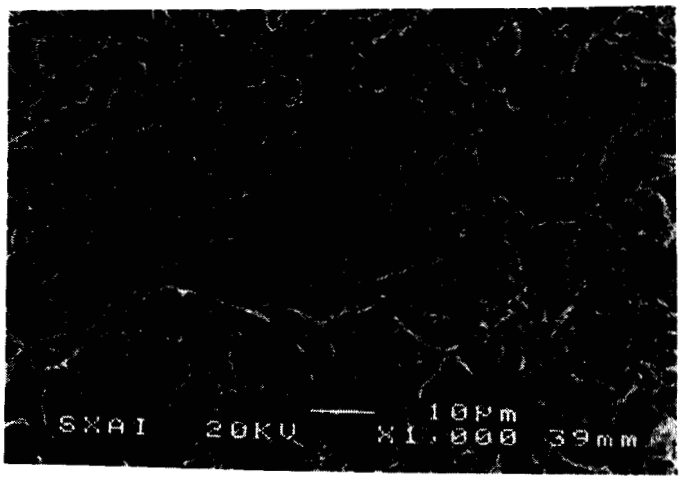

Figure 7: Microscopic fracture mode in steel 1.

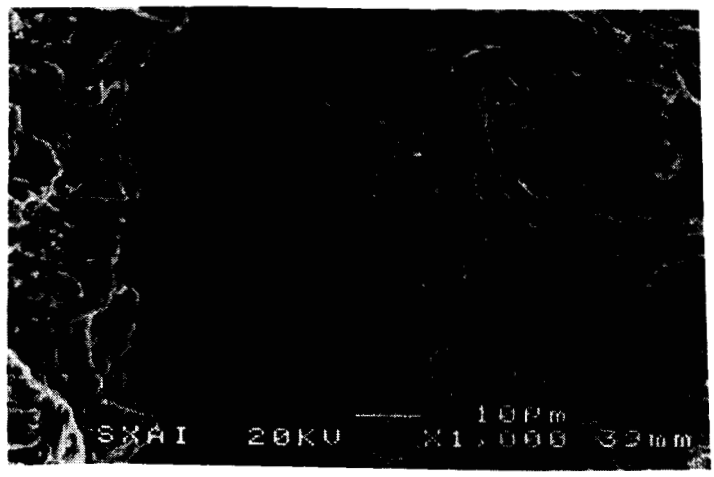

Figure 8: Microscopic fracture mode in steel 5.

MATERIALS SCIENCE APPROACH

In this section a material science approach to the phenomenon of **HAC** in cold drawn eutectoid steel is provided in the form of relationship between the pearlitic microstructure and the macroscopic behaviour, in order to provide insight into the micromechanisms of **HAC** in these materials.

Relationship between Microstructure and Macroscopic HAC Behaviour

Fig *9* plots the orientation angles of the two basic microstructural levels, namely the pearlitic colonies **[4]** and the pearlite lamellae [6], showing a progressive orientation of both microstructural units with cold drawing, as reflected by the evolution of their respective angles in Fig. 9: angle α between the transverse axis of the wire and the major axis of the pearlite colony modelled as an ellipsoid; angle α' between the transverse axis of the wire and the direction marked by the pearlite lamellae in the longitudinal metallographic section. Fig. 9 also shows the variation of the macroscopic crack parameters, the deflection angle θ and the step height ***h,*** cf. Fig. 4. It is seen that the progressive microstructural orientation (at the two levels of colonies and lamellae) clearly influences the angle and height of the fracture step (increasing with the degree of cold drawing). This suggests that the macroscopic **HAC** behaviour **of** the different steels —progressively anisotropic with cold drawing— is a direct consequence of the microstructural evolution towards an oriented arrangement.

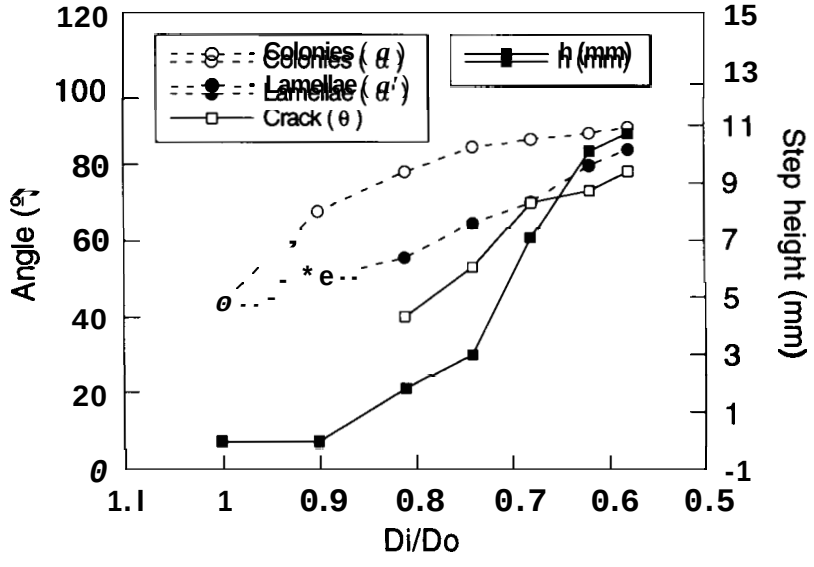

Figure 9: Relationship between the microstructural orientation angles ***a*** and ***a'*** (pearlite colonies and lamellae) and the macroscopic crack parameters (deflection angle θ and step height h) associated with **HAC.**

Micromechanics of Hydrogen Assisted Cracking

A micromechanical model may be proposed to account for the different degrees of cold drawing. It is based on two models proposed previously: (i) the model by Miller and Smith of fracture of pearlitic microstructure by shear cracking **(SC)** of the cementite lamellae [16]; (ii) the mechanism of hydrogen enhanced decohesion (HEDE), a term coined by Gerberich to describe a kind of microscopic fracture mode promoted by hydrogen [17]. For the case of a pearlitic microstructure it would be hydrogen enhanced delamination (or debonding) between two similar microstructural units (colonies or lamellae).

Fig. 10 illustrates the two operative micromechanisms in cold drawn pearlitic steels with certain degree of drawing. In Fig. 10a, it is seen that hydrogen penetration could be easier along the path opened by **SC** of the cementite lamellae. Fig. 10b shows the mechanism of fracture by HEDE. **As** a consequence of the progressive microstructural orientation induced in the material by cold drawing, the micromechanism of fracture evolves form predominant **SC** in slightly drawn steels to predominant HEDE in heavily drawn steels.

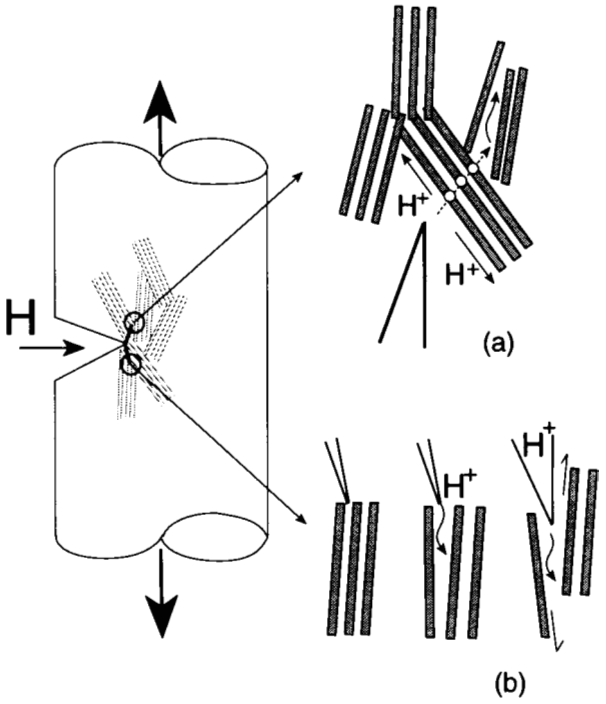

Figure 10: Micromechanical model of **HAC** in steels with certain degree of drawing: (a) hydrogen diffusion in the pearlitic microstructure and penetration along the path opened by a Miller-Smith mechanism of shear cracking **(SC);** (b) fracture by hydrogen enhanced delamination or debonding (HEDE).

CONCLUSIONS

Environmentally assisted cracking of cold drawn eutectoid steel for civil engineering structures was studied in the cathodic regime of hydrogen assisted cracking. The degree of cold drawing (or strain hardening level) was treated as a fundamental variable to analyze the phenomenon.

The resistance of the steel to hydrogen assisted cracking —measured in terms of critical load at the failure instant— does *not* increase by cold drawing, i.e., manufacturing is not beneficial form this viewpoint. However, a certain drawing-induced increase of time to failure seems to exist.

A fracture mechanics approach to the phenomenon was formulated in terms of critical stress intensity factor at the transition from the hydrogen assisted cracking subcritical regime to the final mechanical fracture, showing that the factor K_{HAC} is clearly lower than the fracture toughness of the material in air.

The fractographic analysis demonstrated that the steels exhibit a progressively anisotropic behaviour as the degree of cold drawing increases, with crack deflection and mixed mode propagation in heavily drawn steels as a consequence of the very markedly oriented pearlitic microstructure.

In slightly drawn steels, the microscopic fracture mode resemble tearing topography surface in the subcritical fractured area related to environmentally assisted cracking. This microscopic fracture mode is associated with hydrogen-assisted micro-damage in pearlitic microstructures.

In heavily drawn steels, the microscopic fracture mode is a kind of very deformed tearing topography surface, the deformation axis coincident with the cold drawing direction. This topography is produced as a consequence of the macroscopic crack deflection with mode II propagation.

There is a material science relationship between microstructure and macroscopic fracture behaviour of the steel in conditions of hydrogen assisted cracking, since the progressive microstructural orientation with cold drawing causes the increasingly anisotropic behaviour.

While in slightly drawn steels the predominant micromechanism could be shear cracking in pearlite (Consistent with microscopic fracture by tearing topography surface) it evolves towards hydrogen enhanced delamination of the pearlitic lamellae in the most heavily drawn steels.

Acknowledgements

The financial support of this work by the Spanish CICYT (Grant MAT97-0442) and *Xunta de Galicia* (Grant XUGA 11802B97) is gratefully acknowledged. In addition, the authors wish to express their gratitude to **EMESA TREFILERIA S.A.** (La Coruña, Spain) for providing the steel used in the experimental programme.

REFERENCES

1. Embury, J.D. and Fisher, R.M. (1966) *Acta Metall.* **14,** 147.
2. Langford, G. (1970) *Metall. Trans.* 1,465.
3. Toribio, J. and Ovejero, E. (1997) *Mater. Sci. Engng.* **A234-236**, 579.
4. Toribio, J. and Ovejero, E. (1998) *J. Mater. Sci. Lett.* **17,** 1037.
5. Toribio, J. and Ovejero, E. (1998) *Scripta Mater.* **39,** 323.
6. Toribio, J. and Ovejero, E. (1998) *Mech. Time-Dependent Muter.* **1,** 307.
7. Cherry, B.W. and Price, S.M. (1980) *Corros. Sci.* **20,** 1163.
8. Langstaff, D.C., Meyrick, G. and Hirth, J.P. (1981) *Corrosion* **37,** 429.
9. Parkins, R.N., Elices, M., Sánchez-Gálvez, V. and Caballero, L. (1982) *Corros. Sci.* **22,** 379.
10. Valiente, A. (1980) Ph. D Thesis, Polytechnic University of Madrid.
11. Thompson , A.W. and Chesnutt, J.C. (1979) *Metall. Trans.* **10A**, 1193.
12. Costa, J.E. and Thompson , A.W. (1982) *Metall. Trans.* **13A**, 1315.
13. Toribio, J., Lancha, A.M. and Elices, M. (1991) *Scripta Metall. Mater.* **25,** 2239.
14. Toribio, J., Lancha, A.M. and Elices, M. (1992) *Metall. Trans.* **23A**, 1573.
15. Toribio, J. (1997) *Metall. Trans.* **28A**, 191.
16. Miller, L.E., Smith, G.C. (1979) *J. Iron Steel Inst.* **208,** 998.
17. Gerberich, W.W., Marsh, P, Hoehn, **S.,** Venkataraman, **S,** Huang, H. (1993). In: *Corrosion-Deformation Interactions (CDI'92)*, p. 325, Magnin, T. and Gras, J.M. (Eds.). Les Editions de Physique, Les Ulis.